

Fusion Triple Product and the Density Limit of High-Density Internal Diffusion Barrier Plasmas in LHD

J. Miyazawa¹, R. Sakamoto¹, H. Yamada¹, M. Kobayashi¹, S. Masuzaki¹, T. Morisaki¹,

N. Ohyaabu¹, A. Komori¹, O. Motojima¹, and the LHD experimental group

¹ National Institute for Fusion Science, Toki, Gifu509-5292, Japan

One of the important indices for evaluating the performance of fusion plasmas is a product of the plasma density, n , the energy confinement time, τ , and the plasma temperature, T , that is called the “fusion triple product”, $n\tau T$. High $n_{i0} \tau_E T_{i0}$ of $\sim 1 \times 10^{21} \text{ m}^{-3} \cdot \text{s} \cdot \text{keV}$, where n_{i0} , τ_E and T_{i0} are the central ion density, the energy confinement time, and the central ion temperature, respectively, has been achieved in tokamaks, such as JT-60U [1], JET, TFTR, and DIII-D. Recently, the record of $n\tau T$ in helical plasmas has been increased from $2.2 \times 10^{19} \text{ m}^{-3} \cdot \text{s} \cdot \text{keV}$ to $4.4 \times 10^{19} \text{ m}^{-3} \cdot \text{s} \cdot \text{keV}$ [2], after the discovery of high-density internal diffusion barrier (IDB) plasmas in the Large Helical Device (LHD), where a superdense core of the order of 10^{20} m^{-3} is formed by hydrogen ice pellet injection. To increase $n\tau T$ further, it is of special importance to know the response of $n\tau T$ on various control knobs, *i.e.* the density, the heating power, the magnetic field strength, the magnetic equilibrium, and so on.

The parameter dependence of the energy confinement time has been rigorously studied for both tokamak and helical plasmas. Experimental results suggest that τ_E in toroidal plasmas, independent on the confinement scheme, has the gyro-Bohm like property [3], *i.e.*

$$\tau_E \propto (n_e / P_{\text{tot}})^{-3/5}, \quad (1)$$

where n_e is the electron density and P_{tot} is the total heating power. Using this, the fusion triple product is expressed as below;

$$n\tau T \propto W_p \tau_E \propto (P_{\text{tot}} \tau_E) \tau_E \propto n_e^{1.2} P_{\text{tot}}^{-0.2}, \quad (2)$$

where W_p ($\propto nT$) is the plasma stored energy. This means that one can increase $n\tau T$ by increasing the density and/or decreasing the heating power. On the other hand, the maximum density achievable under a given condition is limited. The density limit in helical plasmas is well reproduced by the Sudo scaling [4] of

$$n_c^{\text{Sudo}} (10^{20} \text{ m}^{-3}) = 0.25 (P_{\text{tot}} B / (a^2 R))^{0.5}, \quad (3)$$

where B , a , R are the magnetic field strength in T, the plasma minor radius in m, and the plasma major radius in m, respectively, and the unit of P_{tot} is MW. As seen in Eq. (3), the

operational density range increases with $P_{\text{tot}}^{0.5}$ in helical plasmas. If we simply substitute $n_e = P_{\text{tot}}^{0.5}$ into Eq. (2), it is expected that

$$n\tau T \propto P_{\text{tot}}^{0.4}. \quad (4)$$

On the contrary to Eq. (2), $n\tau T$ increases with the heating power, in this case.

Hereinafter, the fusion triple product of IDB plasmas in LHD is discussed. The density and the heating power are widely scanned to investigate the parameter dependence of $n\tau T$. Especially, reduction of the heating power after the IDB formation is effective in increasing $n\tau T$, which we call ‘‘annealing’’ operation on the analogy of metallurgy.

The IDB plasmas are formed after n_{e0} is rapidly increased to $10^{20} - 10^{21} \text{ m}^{-3}$ by hydrogen ice pellet injection, where n_{e0} is the central electron density. It is plausible to assume $n_{e0} \sim n_{i0}$ ($Z_{\text{eff}} \sim 1$) and $T_{e0} \sim T_{i0}$ (T_{e0} is the central electron temperature) in the superdense IDB plasmas. Typical waveforms in neutral beam (NB) heated IDB discharges are shown in Fig. 1. In the figure, an annealing discharge (black), where P_{tot} is reduced from $\sim 14 \text{ MW}$ to $\sim 8 \text{ MW}$ after the IDB formation, is compared with high power ($P_{\text{tot}} \sim 14 \text{ MW}$, red) and low power ($P_{\text{tot}} \sim 8 \text{ MW}$, blue) heating discharges. The number of hydrogen pellets and the injection intervals are identical and the temporal behaviour of n_{e0} is similar for the three cases (Fig. 1 (b)). The maximum of n_{e0} is reached just after the pellet injection ($\sim 0.9 \text{ s}$), and then, n_{e0} gradually decreases with a time constant of the order of second. During the density decay phase, T_{e0} once decreased to $\sim 300 \text{ eV}$ gradually increases (Fig. 1 (c)). The

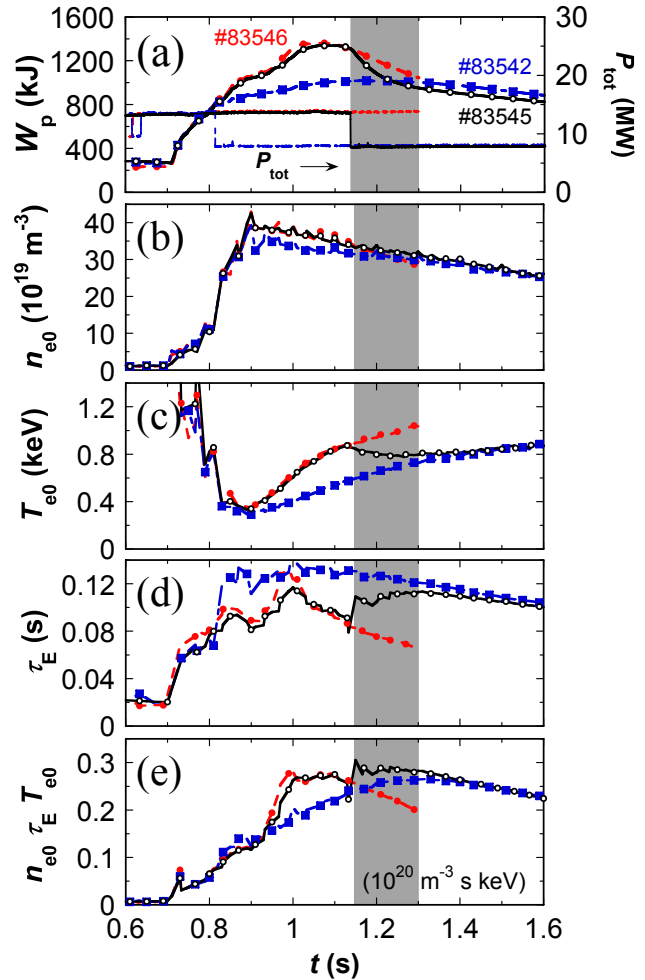


Figure 1. Typical waveforms in an annealing discharge (black), compared with high power (red) and low power (blue) heating discharges. (a) The diamagnetic plasma stored energy, W_p , and the total heating power, P_{tot} , (b) the central electron density, n_{e0} , (c) the central electron temperature, T_{e0} , (d) the energy confinement time, τ_E , and (e) the fusion triple product, $n_{e0} \tau_E T_{e0}$, are shown from top to bottom.

temperature profile that becomes flat or hollow due to the pellet ablation in the plasma core region recovers its parabolic shape as T_{e0} increases. In the case of annealing discharge, T_{e0} stops increasing after the heating power reduction, although the temperature profile continues changing to parabolic. Nevertheless, τ_E defined by

$$\tau_E \equiv W_p / (P_{\text{tot}} - dW_p/dt) \quad (5)$$

increases in this case (Fig. 1 (d)), since the heating power is reduced while the density and the temperature is kept. As a result, the

largest fusion triple product of $n_{e0} \tau_E T_{e0}$ is obtained in the annealing discharge (Fig. 1 (e)).

Results of the P_{tot} scan experiment are summarized in Fig. 2, where $n_{e0} \tau_E T_{e0}$ is plotted against P_{tot} (red filled circles), or the effective total heating power, $P_{\text{tot}} - dW_p/dt$ (blue crosses), which takes the transient effect into account. In both cases, the upper envelope of the data increases as the heating power decreases, which suggests $n \tau T \propto P_{\text{tot}}^{-0.5}$. Qualitatively, the expectation of Eq. (2) predicting a negative power dependence of $n \tau T$ is better than that of Eq. (4) predicting a positive power dependence. However, the negative dependence of $P_{\text{tot}}^{-0.5}$ is much stronger than $P_{\text{tot}}^{-0.2}$ in Eq. (2).

The data shown in Fig. 2 are taken from annealing discharges, where the heating power is reduced after the IDB formation. An excess of the heating power reduction leads to radiative collapse. According to the former study on the density limit in LHD [5], the hot plasma column shrinks inside the last-closed-flux-surface and complete detachment takes place when the edge density, n_e^{edge} , exceeds a value predicted by the Sudo scaling. Then, one should avoid further increase of n_e^{edge} , otherwise the plasma column continues shrinking and radiative collapse will take place. This scenario is independent on the density profile, *i.e.* the density limit in LHD is determined by the local density at the plasma edge [5]. In this study, the modified Sudo scaling, $n_c^{\text{Sudo}^*}$, defined as below is used to take the transient effect into consideration and keep the consistency with τ_E defined by Eq. (5);

$$n_c^{\text{Sudo}^*} (10^{20} \text{ m}^{-3}) = 0.25 ((P_{\text{tot}} - dW_p/dt) B / (a^2 R))^{0.5}, \quad (6)$$

where $P_{\text{tot}} - dW_p/dt$ is used instead of P_{tot} alone. Although both higher density and lower heating

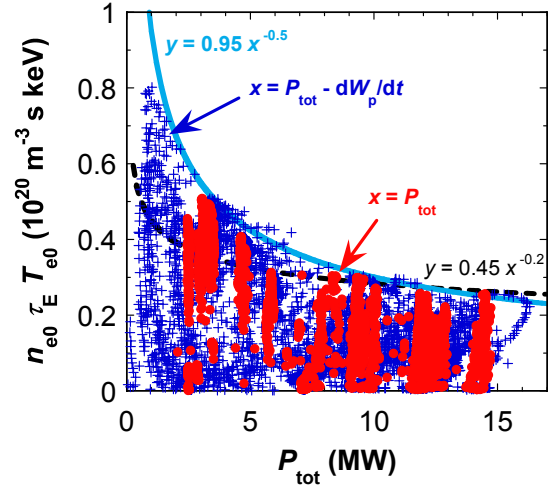


Figure 2. The fusion triple product, $n_{e0} \tau_E T_{e0}$, versus the total heating power, P_{tot} (filled circles), or $P_{\text{tot}} - dW_p/dt$ (crosses).

power are preferable for achieving high $n\tau T$, one should keep a condition for the edge density as below,

$$n_e^{\text{edge}} / n_c^{\text{Sudo}^*} < 1, \quad (7)$$

to avoid radiative collapse. According to the experimental results, $n\tau T$ is proportional to both $n_e^{\text{edge}} / n_c^{\text{Sudo}^*}$ and the peaking factor of the density profile, as long as the parabolic temperature profile is kept. Here, let us define the density peaking factor by $n_{e0} / n_e^{\text{edge}}$, then

$$n_{e0} \tau_E T_{e0} \propto (n_{e0} / n_e^{\text{edge}}) (n_e^{\text{edge}} / n_c^{\text{Sudo}^*}) \propto n_{e0} / n_c^{\text{Sudo}^*}. \quad (8)$$

In Fig. 3, $n_{e0} \tau_E T_{e0}$ is plotted against the right-hand-side term of Eq. (8), $n_{e0} / n_c^{\text{Sudo}^*}$. A linear relation between $n_{e0} / n_c^{\text{Sudo}^*}$ and $n_{e0} \tau_E T_{e0}$ is indeed recognized on the upper envelope of Fig. 3. The upper envelope is composed of the data with parabolic temperature profiles. The ratio of $n_{e0} \tau_E T_{e0} / (n_{e0} / n_c^{\text{Sudo}^*})$ is small when the temperature profile is flat or hollow, which causes the large scatter below the upper envelope in Fig. 3. Returning to Fig. 2, the relatively strong negative power dependence of $n\tau T \propto P_{\text{tot}}^{-0.5}$ is now understood as the consequence of Eq. (8), *i.e.* $n\tau T \propto (n_c^{\text{Sudo}^*})^{-1} \propto P_{\text{tot}}^{-0.5}$.

In summary, the parameter dependence of $n\tau T$ has been studied by applying the annealing operation to high-density IDB plasmas in LHD. To increase $n\tau T$, it is effective to increase the density peaking factor ($n_{e0} / n_e^{\text{edge}}$) within the operational density limit ($n_e^{\text{edge}} / n_c^{\text{Sudo}^*} < 1$). Peaked temperature profiles are also preferable. As long as the temperature profile is parabolic, $n\tau T$ is proportional to $n_{e0} / n_c^{\text{Sudo}^*}$. The largest $n_{e0} \tau_E T_{e0}$ achieved by the annealing operation is $5.1 \times 10^{19} \text{ m}^{-3} \cdot \text{s} \cdot \text{keV}$ ($n_{e0} \sim 4.0 \times 10^{20} \text{ m}^{-3}$, $\tau_E \sim 0.23 \text{ s}$, and $T_{e0} \sim 0.55 \text{ keV}$).

References

- [1] K. Ushigusa *et al.*, Fusion Energy 1996 (Proc. 16th Int. Conf. Montreal, Canada 1996), IAEA, Vol. 1, Vienna, 37 (1997).
- [2] O. Motojima *et al.*, Nucl. Fusion **47**, S668 (2007).
- [3] U. Stroth, Plasma Phys. Control. Fusion **40**, 9 (1998).
- [4] S. Sudo *et al.*, Nucl. Fusion **30**, 11 (1990).
- [5] J. Miyazawa *et al.*, Nucl. Fusion **48**, 015003 (2008).

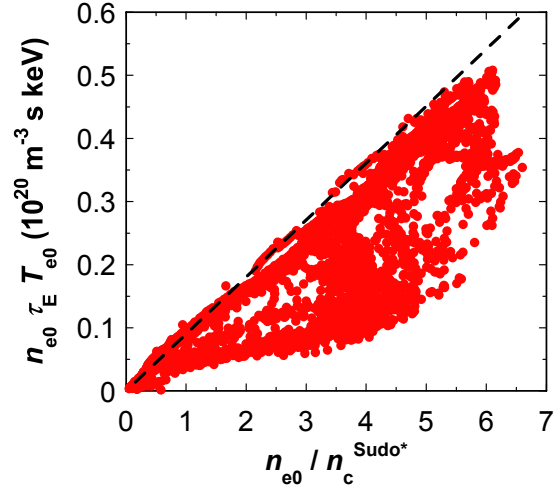


Figure 3. The fusion triple product, $n_{e0} \tau_E T_{e0}$, with respect to $n_{e0} / n_c^{\text{Sudo}^*}$.